JCTC Journal of Chemical Theory and Computation

Article

pubs.acs.org/JCTC

Generalized Valence Bond Description of the Ground States ($X^1\Sigma_g^+$) of Homonuclear Pnictogen Diatomic Molecules: N_2, P_2, and As_2

Lu T. Xu[†] and Thom H. Dunning, Jr.*[,†]

Department of Chemistry, University of Illinois at Urbana−Champaign, 600 South Mathews Avenue, Urbana, Illinois 61801, United States

Supporting Information

ABSTRACT: The ground state, $X^1\Sigma_g^+$, of N_2 is a textbook example of a molecule with a triple bond consisting of one σ and two π bonds. This assignment, which is usually rationalized using molecular orbital (MO) theory, implicitly assumes that the spins of the three pairs of electrons involved in the bonds are singlet-coupled (perfect pairing). However, for a six-electron singlet state, there are five distinct ways to couple the electron spins. The generalized valence bond (GVB) wave function lifts this restriction, including all of the five spin functions for the six electrons involved in the bond. For N_2, we find that the perfect pairing spin function is indeed dominant at R_e but that it becomes progressively less so from N_2 to P_2 and As_2. Although the perfect pairing spin function is still the most important spin function in P_2, the importance of a quasi-atomic spin function, which singlet couples the spins of the electrons in the σ orbitals while high spin coupling those of the electrons in the π orbitals on each center, has significantly increased relative to N_2 and, in As_2, the perfect pairing and quasi-atomic spin couplings are on essentially the same footing. This change in the spin coupling of the electrons in the bonding orbitals down the periodic table may contribute to the rather dramatic decrease in the strengths of the Pn_2 bonds from N_2 to As_2 as well as in the increase in their chemical reactivity and should be taken into account in more detailed analyses of the bond energies in these species. We also compare the spin coupling in N_2 with that in C_2, where the quasi-atomic spin coupling dominants around R_e.

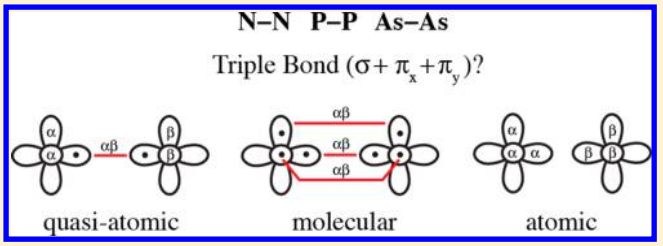

1. INTRODUCTION

One of the goals of modern quantum chemistry is to obtain insights into the nature of chemical bonds: the chemical "objects" that hold atoms together in molecules and give them their three-dimensional structures. Understanding why and how bonds form lays the foundation for the design and control of molecules and molecular processes, an important goal of all chemists. Even though the molecular systems being investigated using high-level quantum chemical techniques have been growing in size, from diatomic molecules a few decades ago to small biomolecular systems today, a basic understanding of the electronic structure of some simple molecules is still unsettled. Diatomic carbon, $C_2(X^1\Sigma_g^+)$, with just two carbon atoms, is a prime example. The nature of the bonding in the ground state of C_2 has long been a subject of interest and, in the past few years, has become a topic of hot debate.[1−6] Using molecular orbital (MO) theory arguments, chemists have traditionally attributed a double bond to C_2,[7] but, recently, others have argued in favor of a triple bond[1] and, later, a quadruple bond,[2] based on detailed valence bond (VB) calculations. The experimental data available on diatomic carbon is, in fact, rather puzzling: C_2 has a bond distance that lies in between that of a double carbon−carbon bond and triple carbon−carbon bond, whereas its bond energy lies between that for a single carbon−carbon bond and a double carbon−carbon bond.

To gain further insights into the nature of the bonding in C_2, we carried out generalized valence bond (GVB) calculations on the ground, $X^1\Sigma_g^+$, state.[8] Surprisingly, we discovered that, for C_2, the GVB wave function with four singlet-coupled electron pairs provides a poor description of the molecule. Instead, we found that C_2 has a traditional σ bond but that the remaining electrons on each of the carbon atoms are antiferromagnetically coupled, i.e., the three other electrons on each carbon atom are high-spin coupled and then the spins of all of the electrons are coupled to give an overall singlet state. This unusual type of bonding is a factor in the unusual properties of the C_2 molecule noted above. It cannot be described by a Hartree−Fock (HF) wave function, and its description by a multiconfiguration self-consistent field (MCSCF) wave function requires a complex mixture of space-spin configurations. On the other hand, this bonding scheme can be straightforwardly described by a GVB wave function. Thus, C_2, a textbook example for teaching about bonding in homonuclear diatomic molecules, turns out to be much different from the simple description derived from an MO diagram.

If the electronic structure of C_2 is so different from that described by MO theory, then what about other molecules, e.g., its neighbor in the periodic table, N_2? Furthermore, are there any systematic changes in the nature of the bonding in the Pn_2

Received: February 4, 2015
Published: April 22, 2015

DOI: 10.1021/acs.jctc.5b00104
J. Chem. Theory Comput. 2015, 11, 2496−2507

homonuclear diatomic molecules progressing down the periodic table, from N_2 to P_2 and As_2? All three of these species are assumed to have one σ and two π bonds, but, given the rather steep decline in the dissociation energies from 228.4 kcal/mol in N_2 to 116.9 kcal/mol in P_2 and 92.0 kcal/mol in As_2, is this assignment justified for all of these species?[9] In addition, why are the reactivities of the three molecules so different? N_2 is chemically inert, but P_2 is highly reactive, with pyrolysis of white phosphorus, tetrahedral P_4, yielding the chemically unstable gaseous P_2.[10,11] Diarsenic, As_2, is also highly reactive and exists in the vapor phase only at high temperatures.[12] Even the tetrahedral As_4 is chemically unstable, readily transforming into gray arsenic.[13] To address these questions, we report GVB as well as more accurate calculations on the ground, $X^1\Sigma_g^+$, states of the N_2, P_2, and As_2 molecules. The goal is to examine the nature of the bonding in these molecules and to determine if it changes from N_2 to P_2 and As_2. We also compare the bonding in N_2 with that in C_2, a comparison that reinforces the unusual nature of the bonding in C_2.

In the next section (Section 2), we briefly discuss the theoretical and computational methods that we will use. In Section 3, we discuss the results of the calculations on N_2, comparing the HF and GVB descriptions of N_2 as well as the GVB description of N_2 with that of C_2 and then the GVB description of N_2 with those of P_2 and As_2. Finally, in the last section (Section 4), we summarize our findings. The present work may be considered as an elaboration of the work of Dunning et al. on N_2 that was reported in the late 1970s.[14]

2. THEORETICAL AND COMPUTATIONAL METHODS

2.1. Computational Details. The potential energy curves, equilibrium geometries, dissociation energies, and other properties of the ground, $X^1\Sigma_g^+$, states of N_2, P_2, and As_2 were computed at various levels of theory: HF, GVB,[15,16] valence CASSCF (with an ns + np active space)[17−20] as well as the corresponding multireference configuration interaction (MRCI)[21−23] with the quadruples correction (+Q),[24] and coupled cluster singles and doubles with perturbative triples [CCSD(T)].[25−27] An augmented correlation consistent basis set of quadruple-ζ quality (aug-cc-pVQZ)[28] was used for nitrogen, the corresponding d-function augmented set [aug-cc-pV(Q+d)Z][29] was used for phosphorus, and the augmented correlation consistent basis set of quadruple-ζ quality with pseudopotential (aug-cc-pVQZ-PP)[30] was used for arsenic. All of the calculations in this work were performed with the Molpro suite of quantum chemical programs.[31,32]

2.2. GVB Wave Functions for the Ground States of the Pn_2 Molecules. As a reference wave function, the GVB wave function strikes an appealing balance between accuracy and interpretability. The GVB wave function is more accurate than a HF wave function, including most, if not all, nondynamical atomic and molecular correlation effects, which are neglected in HF theory. Since the orbitals are optimized, the GVB wave function also includes important mean-field effects, e.g., changes in orbital extent as well as hybridization, delocalization, and so on. The GVB wave function takes into account all of the possible spin couplings for the electrons in the active orbitals, so it does not predetermine a specific spin function. Finally, the GVB wave function can be interpreted in terms of concepts familiar to many chemists, although new concepts have also arisen, such as recoupled pair bonding.[33−35] For a more detailed description of the GVB wave function and its analysis, refer to refs 34 and 35.

The un-normalized GVB wave function for the ground state ($X^1\Sigma_g^+$) of the homonuclear pnictogen diatomic molecules (Pn_2) is

$$\Psi_{\mathrm{GVB}}[\mathrm{Pn}_2(X^1\Sigma_g^+)] = \hat{a}(core)\phi_{v1}\phi_{v1}\phi_{v2}\phi_{v2}\varphi_{a1}\varphi_{a2}\varphi_{a3}\varphi_{a4}\varphi_{a5}\varphi_{a6}\alpha\beta\alpha\beta\Theta_{0,0}^6 \quad (1)$$

In eq 1, $\hat{a}$ is the antisymmetrizer ensuring that the wave function satisfies the Pauli principle, and the doubly occupied core orbitals and associated spin functions of the nitrogen, phosphorus, and arsenic atoms are denoted by ($core$). The two doubly occupied valence orbitals (ϕ_{v1}, ϕ_{v2}) correlate with the ns orbitals of the two atoms, whereas the six active orbitals (φ_{a1}−φ_{a6}) correlate with the np orbitals of the two atoms (n = 2−4). The doubly occupied orbitals in eq 1 can be taken to be orthogonal to each other, and the singly occupied orbitals can be taken to be orthogonal to the doubly occupied orbitals without changing the wave function. The singly occupied active orbitals are, in general, nonorthogonal. The symmetry properties of the GVB wave function for N_2, as well as C_2H_2, have been discussed in detail by Penotti and Cooper.[36]

The product of spatial orbitals in eq 1 is multiplied by an $\alpha\beta\alpha\beta$ spin function for the four electrons in the two doubly occupied ns lone pair orbitals times a spin function, $\Theta_{0,0}^6$, for the electrons in the six active orbitals, which are the np bonding orbitals. The latter is a linear combination of spin functions representing the five linearly independent ways to couple the spins of the six electrons in the active orbitals to obtain a singlet state, i.e.

$$\Theta_{0,0}^6 = \sum_{k=1}^{5} c_{0,0;k}\Theta_{0,0;k}^6 \quad (2)$$

We use the Kotani[37−39] spin functions in eq 2. These functions are denoted symbolically by ($\Theta_{0,0;1} \equiv \alpha\alpha\alpha\beta\beta\beta$), ($\Theta_{0,0;2} \equiv \alpha\alpha\beta\alpha\beta\beta$), ($\Theta_{0,0;3} \equiv \alpha\beta\alpha\alpha\beta\beta$), ($\Theta_{0,0;4} \equiv \alpha\alpha\beta\beta\alpha\beta$), and ($\Theta_{0,0;5} \equiv \alpha\beta\alpha\beta\alpha\beta$), and their detailed functional forms are given in the Supporting Information. The Kotani spin functions are orthonormal, so the contribution of a given spin function to the GVB wave function is the square of its coefficient (the sum of the weights is unity). Raos et al.[40] discussed the use of alternate representations of the spin functions, including the use of Serber spin functions in C_2.

In exploring the nature of the bonding in the Pn_2 molecules, we will use an important property of the GVB wave function: the invariance of the wave function to a reordering of the orbitals. Although the full GVB wave function and energy do not change if the ordering of the active orbitals is changed, the coefficients of the various spin functions $\{c_{0,0;k}\}$ in eq 2 will change. By reordering the active orbitals, we can probe different ways to describe the spin coupling of the electrons in those orbitals. For example, if the orbital pairs describing the three bonds in Pn_2 are arranged sequentially, referred to as the molecular ordering, then the weight of the ($\alpha\beta\alpha\beta\alpha\beta$) spin function, $\Theta_{0,0;5}^6$, which is the perfect pairing (PP) spin function, is a measure of how well the molecule is described as having three traditional covalent bonds. This concept was, in fact, used in our studies of C_2 to identify a better way to describe the bonding in this molecule.[8] There, we found that the quasi-atomic ordering and its corresponding spin function provided a better description of C_2 than did the molecular ordering and the perfect pairing spin function (although neither alone was truly satisfactory). We will use this freedom again in the current article to gain insights into the nature of the bonding in N_2, P_2, and As_2 and how the bonding changes from N_2 to P_2 and As_2.

DOI: 10.1021/acs.jctc.5b00104
J. Chem. Theory Comput. 2015, 11, 2496−2507

Although we will use the GVB notation to refer to the calculations presented here, the fully optimized GVB wave function is identical to the spin-coupled valence bond (SCVB) wave function of Gerratt, Cooper, Karadakov, Raimondi, and co-workers.[41−43] The calculations reported herein were, in fact, made possible by the methodology developed by Thorsteinsson and Cooper and implemented in the CASVB module in Molpro.[44−47]

3. RESULTS AND DISCUSSION

In this section, we first discuss the results of the calculations on N_2 (Section 3.1) and then compare the GVB results on N_2 with those from GVB calculations on C_2 (Section 3.2). Finally, we discuss P_2 and As_2 (Section 3.3).

3.1. Electronic Structure of N_2. The computed equilibrium geometries and energetics of the ground state, $X^1\Sigma_g^+$, of N_2 are reported at various levels of theory in this section. The GVB wave function of N_2 is then analyzed to determine the nature of the bonding in this prototypical, multiply bonded species. It is shown that the orbitals, orbital overlaps, and spin function weights as a function of the internuclear distance (R) provide valuable insights into how the bonds form as well as the nature of the bonding at the equilibrium bond distance. Finally, the results of selected GVB calculations on N_2 are compared with the HF calculations.

3.1.1. Calculated Potential Energy Curves and Spectroscopic Constants of N_2. Figure 1 shows the calculated potential energy curves for $N_2(X^1\Sigma_g^+)$ at the HF, GVB, valence-CASSCF, and MRCI+Q levels. Table 1 summarizes the computed spectroscopic constants for the ground state of N_2 using these methods as well as the CCSD(T) method.

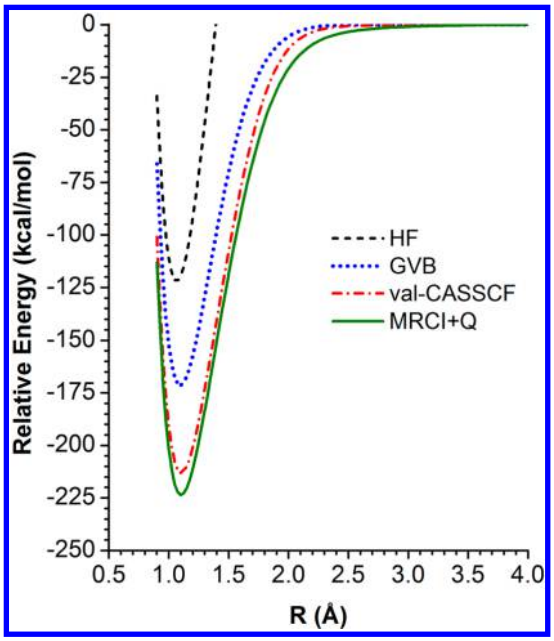

Figure 1. Potential energy curves of $N_2(X^1\Sigma_g^+)$ at four levels of theory; the CCSD(T) curve is very close to the MRCI+Q curve around R_e. Basis set: aug-cc-pVQZ.

The experimental equilibrium bond distance (R_e) of N_2 is 1.098 Å, with which the GVB, valence-CASSCF, MRCI+Q, and CCSD(T) computed bond distances are in good agreement. The GVB calculations predict an R_e that is too short by just 0.002 Å, whereas the MRCI+Q and CCSD(T) calculations predict an R_e that is too long by just 0.003 Å. The valence-CASSCF calculations have a slightly larger error of +0.006 Å, whereas the error in the HF calculations is much larger, −0.032 Å.

Table 1. Equilibrium Bond Distances (R_e), Dissociation Energies (D_e), Harmonic Vibrational Frequencies (ω_e), and Total Energies (E_e) for the Ground ($X^1\Sigma_g^+$) State of N_2[a]

method	R_e (Å)	D_e (kcal/mol)	ω_e (cm^{-1})	E_e (au)
HF	1.066	122.04	2728.9	−108.994933
GVB	1.096	171.38	2369.7	−109.073564
val-CASSCF	1.104	213.17	2339.2	−109.140166
MRCI+Q	1.101	223.56	2339.9	−109.406619
CCSD(T)	1.101	224.05	2354.5	−109.407243
Expt[b]	1.098	228.4	2358.6	

[a]Basis set: aug-cc-pVQZ. [b]Ref 9.

The binding energy (D_e) computed at the CCSD(T) level is 224.05 kcal/mol, and at the MRCI+Q level, it is only slightly less, 223.56, both of which are very close to the experimental value, 228.4 kcal/mol (for a more detailed discussion of the effects that must be included to predict an accurate dissociation energy for N_2, see ref 48). The GVB wave function predicts D_e = 171.38 kcal/mol, or 75% of the experimental dissociation energy. The HF method predicts a bond energy of 122.04 kcal/mol, or just 53% of the dissociation energy, whereas the valence CASSCF (val-CASSCF) method predicts 93% of the dissociation energy (213.17 kcal/mol). The energy of the val-CASSCF wave function is usually taken as the reference point for defining the nondynamical correlation energy for a molecule. So, this result implies that the *dynamical correlation energy* contribution to D_e is very small in N_2, on the order of 15 kcal/mol, a rather surprising result given that the electrons are more densely packed in the molecule than in the atoms. If, instead, the GVB wave function is used as the reference for the definition of nondynamical correlation, then the dynamical correlation contribution to D_e is 57 kcal/mol in N_2. This can be compared to a corresponding value of 33 kcal/mol in C_2.[8] Since the number of valence electrons is larger in N_2 (10) than in C_2 (8) and the internuclear distance is shorter, we would expect dynamical correlation to make a larger contribution to the dissociation energy in diatomic nitrogen than in diatomic carbon to be in line with this result. The situation is even more puzzling if the val-CASSCF wave function is used as the reference for defining the nondynamical correlation energy in C_2. In this case, the dynamical correlation energy contribution to the dissociation energy of C_2 would be just a couple of kcal/mol, which is unusual to say the least.

3.1.2. GVB Description of the Electronic Structure of N_2. The GVB wave function is fully defined by the orbitals and spin coupling coefficients. Changes in the active orbitals and spin coupling coefficients involved in bonding from $R = \infty$ to $R = R_e$ provide insights into the primary effects of molecular formation. The corresponding changes in the doubly occupied valence orbitals, which are not directly involved in bonding, reveal the secondary effects of molecular formation.

Orbitals and Orbital Overlaps. Figure 2 shows the singly occupied GVB active orbitals $\{\varphi_{ai}\}$ in the molecular ordering as well as the doubly occupied valence orbitals (ϕ_{vi}) of N_2 as a function of ΔR, where $\Delta R = R - R_e$, with R_e being the MRCI optimized bond distance, 1.101 Å. Only the in-plane $2p\pi_x$-like orbitals (φ_{a3}, φ_{a4}) are shown; the $2p\pi_y$-like orbitals (φ_{a5}, φ_{a6}) are perpendicular to the plane but are otherwise exactly the same as (φ_{a3}, φ_{a4}). Note that since the lone pair orbitals (ϕ_{v1}, ϕ_{v2}) are

DOI: 10.1021/acs.jctc.5b00104
J. Chem. Theory Comput. 2015, 11, 2496−2507

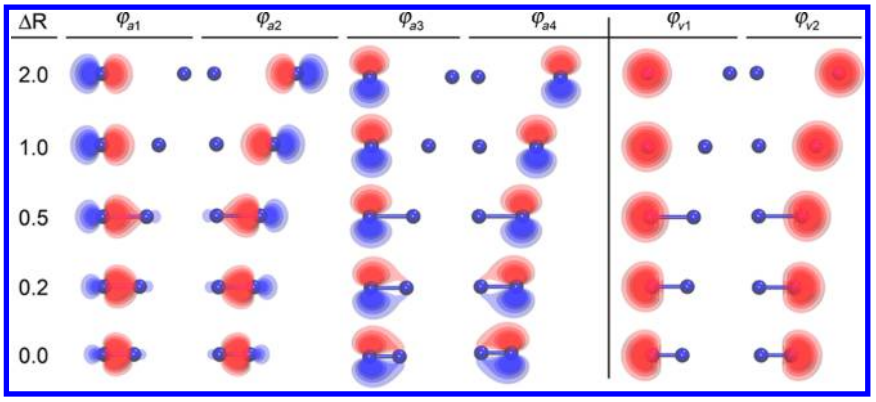

Figure 2. GVB orbitals of $N_2(X^1\Sigma_g^+)$ as a function of ΔR; $\Delta R = R - R_e$, R_e = 1.101 Å. GVB active orbitals are on the left side of the vertical divider, and doubly occupied valence orbitals are on the right side. Basis set: aug-cc-pVQZ.

doubly occupied, they could be transformed to σ_g and σ_u orbitals without changing the GVB wave function.

At large separation, ΔR = 2.0 Å, (φ_{a1}, φ_{a2}) are essentially the nitrogen $2p_z$ orbitals, (φ_{a3}, φ_{a4}) are the nitrogen $2p\pi_x$ orbitals, and (φ_{v1}, φ_{v2}) are the 2s orbitals on the left and right nitrogen atoms. As ΔR decreases, the σ bonding orbitals (φ_{a1}, φ_{a2}) hybridize and delocalize onto the other nitrogen atom, enhancing the overlap and increasing the bond strength. Similar changes occur in the π bonding orbitals (φ_{a3}, φ_{a4}), although to a lesser extent.

The overlaps between the σ and π bonding orbitals are plotted in Figure 3. As expected from the spatial orientation of the

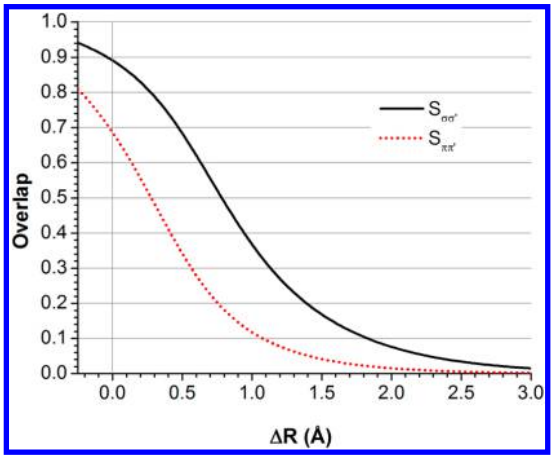

Figure 3. Orbital overlaps for the σ and π bonding orbitals of $N_2(X^1\Sigma_g^+)$ as a function of ΔR; $\Delta R = R - R_e$; R_e = 1.101 Å.

orbitals, the overlap between the σ bonding orbitals, S_{12}, is greater than the overlap between the π bonding orbitals, S_{34}, at all distances. As ΔR decreases, S_{12} increases more rapidly than S_{34}, although the curves have the same general shape. At R_e (indicated by the vertical line in Figure 3 at ΔR = 0.0), S_{12} = 0.89 and S_{34} = 0.69, which is consistent with the fact that σ bonds are deemed to be stronger than π bonds. If ΔR continues to decrease, becoming negative, then the overlaps keep increasing, with the increase in the overlap of the σ bonding orbitals (S_{12}) continuing but at a decreased rate.

The changes in the orbitals derived from the nitrogen 2s atomic orbitals are equally profound. As ΔR decreases, the doubly occupied valence orbitals (φ_{v1}, φ_{v2}) move in the opposite direction to the σ bond pair (φ_{a1}, φ_{a2}), polarizing out of the bonding region. This is a result of Pauli repulsion between the forming bond pair and the nitrogen 2s pairs and results in a buildup of charge density in the nonbonding region behind each of the nitrogen atoms. Thus, a map of the density difference between N_2 and two $N(^4S)$ atoms at R_e will show two positive regions: one between the two nitrogen atoms as a result of bond formation and one behind each of the nitrogen atoms as a result of the 2s orbitals polarizing out of the bonding region. The buildup of charge between the two nitrogen atoms will be less than expected because this region is losing density as the nitrogen 2s orbitals polarize out of the bond region.

Spin Function Weights. As noted above, different active orbital orderings will change the coefficients of the spin eigenfunctions. If the ($\alpha\beta\alpha\beta\alpha\beta$) spin function, Θ_S, is combined with an orbital ordering that lists the σ and π bond pairs sequentially, then the resulting GVB configuration, the perfect pairing configuration, is dominant around the equilibrium geometry for many molecules. (Henceforth, we will drop the S,M subscripts for both $\Theta_{S,M;k}$ and $c_{S,M;k}$.) This is the molecular ordering denoted in Table 2 for N_2. For N_2 at R_e, we find that c_S =

Table 2. Important Orbital Orderings and Associated Dominant Symbolic Spin Functions for Homonuclear Pnictogen Diatomic Molecules: N_2, P_2, and As_2[a]

ordering	*a*1	*a*2	*a*3	*a*4	*a*5	*a*6	symbolic spin function
molecular	$2p_{zA}$	$2p_{zB}$	$2p_{xA}$	$2p_{xB}$	$2p_{yA}$	$2p_{yB}$	$\alpha\beta\alpha\beta\alpha\beta$
quasi-atomic	$2p_{zA}$	$2p_{zB}$	$2p_{xA}$	$2p_{yA}$	$2p_{xB}$	$2p_{yB}$	$\alpha\beta\alpha\alpha\beta\beta$
atomic	$2p_{zA}$	$2p_{xA}$	$2p_{yA}$	$2p_{zB}$	$2p_{xB}$	$2p_{yB}$	$\alpha\alpha\alpha\beta\beta\beta$

[a]A and B are labels for the two nitrogen atoms and z is the intermolecular axis. For the detailed form of the symbolic spin functions, see the Supporting Information.

0.959 and w_S = 0.919 for this ordering and spin function, indicating that N_2 does indeed have a well-defined set of singlet-coupled pairs: one σ bond and two π bonds. This is assumed to be the case in HF theory, but in GVB theory, it is not required; rather, it is a direct result of using the variational principle to determine the optimum wave function. If we optimize the orbitals in a GVB wave function with $\Theta_{0,0} \equiv \Theta_S$, then the energy increases by just 4.15 kcal/mol, which is a direct measure of the impact of forcing the electron pairs in N_2 to be perfectly paired. We refer to this type of wave function as a restricted GVB (rGVB) wave function.

DOI: 10.1021/acs.jctc.5b00104
J. Chem. Theory Comput. 2015, 11, 2496−2507

In Figure 4, we plot the weights of the five spin functions for $N_2(X^1\Sigma_g^+)$ as a function of $\Delta R = R - R_e$ (R_e = 1.101 Å) for the

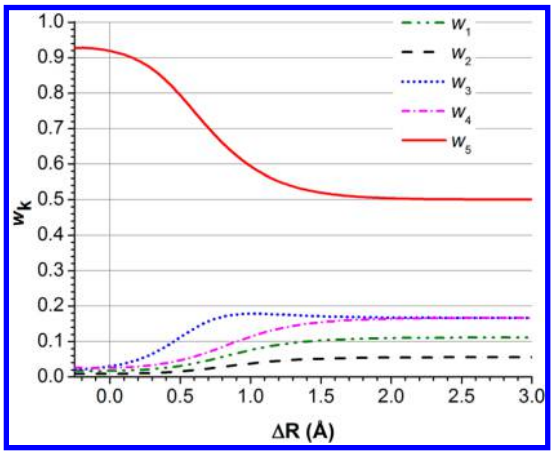

Figure 4. Weights of the five spin functions of $N_2(X^1\Sigma_g^+)$ for the molecular ordering as a function of ΔR; $\Delta R = R - R_e$, R_e = 1.101 Å.

molecular ordering. At $R = \infty$, the weight of the perfect pairing spin function, Θ_5, is 0.500, as is the sum of the weights of the other four spin functions. This combination of spin functions is required to represent the GVB wave function for the separated atoms, $N(^4S) + N(^4S)$, if the molecular ordering is used for the orbitals. As ΔR decreases, w_5 increases and w_1–w_4 decrease. As might be expected, the weight of the spin function that has the σ orbitals (φ_{a1}, φ_{a2}) coupled into a singlet, w_3 ($\Theta_3 \equiv \alpha\beta\alpha\alpha\beta\beta$), decreases less rapidly that the weights of the other spin functions.

There are two other orbital orderings and corresponding spin functions that are important for the Pn_2 series. These are also listed in Table 2. The second orbital ordering is the quasi-atomic ordering, which places the two σ bonding orbitals first, the two π orbitals on one of the atoms next, and the two π orbitals on the other atom last. When combined with Θ_3 ($\alpha\beta\alpha\alpha\beta\beta$), the resulting rGVB(*quasi-atomic*) wave function describes a traditional, singlet-coupled σ bond with the electrons in the more weakly interacting π orbitals on the two centers being antiferromagnetically coupled as they are in the atoms. This is the type of spin coupling that was found to be optimum for C_2 at R_e. The third ordering lists all of the orbitals on one atom first and all of the orbitals on the other atom next. When this ordering is combined in an rGVB wave function with Θ_1 ($\alpha\alpha\alpha\beta\beta\beta$), all of the electrons on the two atoms are antiferromagnetically coupled. This is the atomic ordering. The corresponding rGVB(*atomic*) wave function is equivalent to a spin-extended Hartree–Fock (SEHF) wave function.[49]

In Table 3, we list the GVB energies and spin coupling weights for the three orbitals orderings for the N_2 molecule at R_e. To quantify the impact of restricting the spin function associated with a particular orbital ordering, we optimized the rGVB wave functions that combined the given orbital ordering with the optimum spin function for that ordering: Θ_5 for the molecular ordering, Θ_3 for the quasi-atomic ordering, and Θ_1 for the atomic ordering. We also list $\Delta E_{rGVB} = E_{rGVB} - E_{GVB}$, where E_{rGVB} is the energy obtained when the orbitals for the given ordering is combined with the dominant spin function for that ordering and the orbitals are optimized. As noted above, the energy of the rGVB wave function with the molecular ordering, rGVB(*molecular*), which is the GVB(PP) wave function, lies just 4.15 kcal/mol above the energy of the full GVB wave function at

Table 3. GVB and rGVB Energies, Spin Function Weights, Orbital Overlaps, and Energy Differences for the Three Orbital Orderings for $N_2(X^1\Sigma_g^+)$ at R_e = 1.101 Å[a]

	molecular	quasi-atomic	atomic
E_{GVB} (au)	−109.073480		
w_1	0.0169	0.0169	0.7722
w_2	0.0085	0.0339	0.0298
w_3	0.0300	0.8407	0.0895
w_4	0.0254	0.0000	0.0814
w_5	0.9192	0.1085	0.0271
$S_{\sigma\sigma'}$		0.89	
$S_{\pi\pi'}$		0.69	
E_{rGVB} (au)	−109.066870	−109.058550	−109.056666
$S_{\sigma\sigma'}$	0.89	0.89	0.97
$S_{\pi\pi'}$	0.69	0.75	0.74
ΔE_{rGVB} (kcal/mol)	4.15	9.37	10.55

[a]See Table 2 for the three orbital orderings.

the R_e of N_2. The other orbital orderings/spin functions are less favorable: the rGVB(*quasi-atomic*) wave function is in error by 9.37 kcal/mol, whereas the error in the rGVB(*atomic*) wave function is 10.55 kcal/mol.

Although a visual examination of the orbitals associated with the three rGVB wave functions shows some differences, more revealing are the changes in the overlaps for the three sets of orbitals. Given the close similarity of the GVB and rGVB(*molecular*) wave functions at R_e, it is not surprising that the overlaps are essentially the same for these two sets of orbitals, 0.89 (σ) and 0.69 (π). For the other rGVB wave functions, significant changes in the overlaps occur only when the spin coupling of the associated orbitals changes. Thus, the singlet-coupled σ pair in the rGVB(*quasi-atomic*) wave function has essentially the same overlap as in the rGVB(*molecular*) wave function (0.89), but there is a significant increase in the overlap of the π bonding pairs, to 0.75. Similarly, we find that there is a significant increase in the overlap of the σ orbital pair in the atomic wave function, to 0.97. In fact, in the atomic wave function, the σ pair is almost a doubly occupied orbital, in which case $S_{\sigma\sigma'} \equiv 1$. This increase in the overlaps compensates for the less favorable spin coupling of the electrons in the associated orbitals.

As shown in Figure 4, the weights of the five spin functions for the molecular ordering vary as a function of ΔR. This is also the case for the quasi-atomic and atomic orderings of the orbitals. (Refer to Figures S1 and S2 in the Supporting Information for a detailed discussion.) Figure 5 is a plot with the weights of the three dominant spin functions for the three orbital orderings as a function of ΔR. (Note that because of the different orbital orderings used in the three GVB wave functions these weights do not sum to 1.) At large distance, $\Delta R \geq 3.0$ Å, the dominant spin coupling for the atomic ordering has a weight of 1.00, that for the quasi-atomic ordering has a smaller weight of 0.67, and the perfect pairing spin function for the molecular ordering has the smallest weight at 0.50. As ΔR decreases, the weight of the atomic coupling decreases continuously, while the weight of the perfect pairing coupling increases continuously. On the other hand, the weight of the quasi-atomic coupling increases initially, reaching a maximum at $\Delta R \approx 0.45$ Å, and then decreases. Thus, the bonding in N_2 can be partitioned into three regions where each of the three spin functions dominates. Near R_e, the perfect pairing with three singlet-coupled pairs dominates; at large distances, the atomic coupling dominates; and at an intermediate distance,

DOI: 10.1021/acs.jctc.5b00104
J. Chem. Theory Comput. 2015, 11, 2496–2507

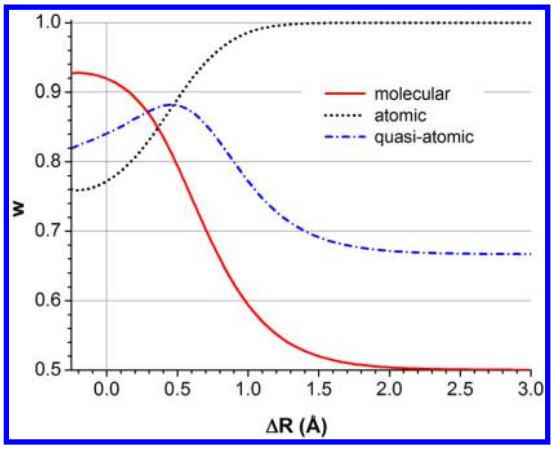

Figure 5. Dominant spin coupling weights for the three different orbital orderings of the $X^1\Sigma_g^+$ state of N_2 as a function of ΔR; $\Delta R = R - R_e$, R_e = 1.101 Å.

when $\Delta R \approx 0.3-0.5$ Å, the quasi-atomic coupling function with one singlet-coupled pair dominates.

3.1.3. Comparison of the GVB and HF Descriptions of N_2. The HF wave function is not able to describe bond breaking in N_2, so the comparison of the GVB and HF wave functions will be restricted to R_e. As can be seen in Table 1, all of the computed spectroscopic constants are predicted much more accurately by GVB theory than HF theory: R_e improves by 0.030 Å, D_e improves by 49.34 kcal/mol, and ω_e improves by 359.2 cm^{-1}. In fact, substantial improvements are to be expected in multiply bonded systems because the π pairs in multiply bonded systems are not well described by a HF wave function.

The results of HF and selected GVB calculations at R_e = 1.101 Å are summarized in Table 4. At this distance, the GVB energy is

Table 4. Comparison of GVB and HF Descriptions of $N_2(X^1\Sigma_g^+)$ at R_e = 1.101 Å[a]

	active space	E_e	ΔE_e
HF	none	−108.990787	0.0
GVB	2 (σ)	−109.003496	−7.97
GVB	4 (π)	−100.056839	−41.45
GVB	6 (σ,π)	−109.073481	−51.89

[a]Total energies, E_e, in hartrees; energy differences, ΔE_e, in kcal/mol.

51.89 kcal/mol below the HF energy (the energy difference is less at the optimum R_e's for the two wave functions; see Table 1). To better understand the source of the errors in the HF wave function relative to the GVB wave function, we performed two GVB calculations that limited the number of active orbitals in the calculation. In the first case, we doubly occupied the σ bonding orbitals, describing the four electrons in the π orbitals using a GVB wave function. This wave function gave an energy that was 41.45 kcal/mol below the HF energy (10.44 kcal/mol above the GVB energy). In the second case, we doubly occupied the π bonding orbitals, describing the σ bonding orbitals by a GVB pair. This wave function gave an energy that was only 7.97 kcal/mol below the HF energy (43.92 kcal/mol above the GVB energy). Clearly, the double occupancy restriction is far more deleterious for the π orbitals (20.72 kcal/mol per pair) than for the σ orbitals (7.97 kcal/mol per pair). This finding was expected: the overlap of the σ orbitals (0.89) is much greater than that of the π orbitals (0.69), and the closer the overlap is to 1, the more accurate the HF description will be.

The GVB wave function includes all five spin couplings associated with the six electrons involved in bonding in N_2. The rGVB(*molecular*)/GVB(PP) wave function uses only the perfect pairing spin function and, thus, is closely related to the HF wave function; it represents each of the doubly occupied bonding molecular orbitals as a pair of GVB orbitals in which the spins of the electrons are also singlet-coupled. The GVB(PP) energy lies 47.74 kcal/mol below the HF energy and just 4.15 kcal/mol above the GVB energy at R_e = 1.101 Å. Thus, around R_e, the major error is associated with the double occupancy requirement, not in the limitation to the perfect pairing spin function.

3.2. Comparison of the GVB Descriptions of N_2 and C_2. As shown above, around its equilibrium geometry, $N_2(X^1\Sigma_g^+)$ is well described by a wave function that is a product of three singlet-coupled pairs corresponding to one σ and two π bonds. The perfect pairing weight, $w_{PP}(\Theta_S)$, is 0.919, with the energy penalty associated with using only this spin coupling being a rather modest 4.15 kcal/mol. In contrast, the GVB wave function for $C_2(X^1\Sigma_g^+)$ is not at all well described by a product of four electron pairs: w_{PP} = 0.669, with the GVB(PP) wave function having an energy that is 20.42 kcal/mol above the full GVB energy. We found that the best single GVB configuration for C_2 corresponded to a single σ bond with the remaining three electrons on each of the carbon atoms antiferromagnetically coupled. The corresponding optimum rGVB(*quasi-atomic*) wave function has an energy that is 10.85 kcal/mol above the full GVB energy. However, the energy difference associated with the quasi-atomic description of C_2 is still $2^1/_2$ times the error associated with the perfect pairing description of N_2. So, this single GVB configuration is not totally adequate for C_2 either. In fact, as we showed in our earlier paper, the electronic structure of C_2 is quite complicated: an accurate GVB wave function consists of a combination of both the quasi-atomic and molecular configurations. Also, as noted in our earlier paper, the reason for the decreased importance of the perfect pairing function is straightforward: singlet coupling the four electrons in the σ orbitals in C_2 leads to strong Pauli repulsions between the two pairs. This is the same reason that Be_2 is barely bound (2.7 kcal/mol[50]) and B_2 is weakly bound (69.6 kcal/mol[9]).

The above interpretation of the nature of the bonding in C_2 has recently been criticized by Danovich et al.[6] They noted that delocalization of the GVB orbitals results in the inclusion of ionic character in the wave function and claimed that, in molecules with multiple bonds, the result would be a systematic bias against the perfect pairing spin coupling. To support this argument, they cited the results of the calculations of Goodgame and Goddard on Cr_2.[51,52] We believe that the situation is more complicated than what this argument implies. Although dynamical electron correlation may well affect the contribution of the perfect pairing spin coupling in a molecule relative to the other spin couplings, it is not clear that this would result in a systematic bias for the perfect pairing spin function. In fact, the present calculations on N_2, which show that the perfect pairing configuration is dominant around R_e for this multiply bonded molecule, provide a strong counter argument.

3.3. Comparison of the GVB Descriptions of N_2 with P_2 and As_2. In this section, the P_2 and As_2 molecules will be discussed and compared to N_2. As the second- and third-row homologues of N_2, P_2 and As_2 have longer bond distances and much weaker bond energies. An over-riding question is whether the bonding in P_2 and As_2 is the same as that in N_2 and, if not, how do they differ?

DOI: 10.1021/acs.jctc.5b00104
J. Chem. Theory Comput. 2015, 11, 2496−2507

3.3.1. Potential Energy Curves and Spectroscopic Constants of P_2 and As_2. Table 5 summarizes the calculated properties of the ground states of P_2 and As_2 obtained with various theoretical methods, and Figure 6 is a composite plot of the calculated GVB and MRCI+Q potential energy curves for the three Pn_2 molecules. Two general trends are obvious: for all theoretical methods, the equilibrium distances (R_e) increase and the binding energies (D_e) decrease down the periodic table, in agreement with experimental results and expectations. For P_2, the calculated bond length at the CCSD(T) level is 1.902 Å with a binding energy of 112.99 kcal/mol. For As_2, the corresponding numbers are 2.120 Å and 87.01 kcal/mol. Both of these results are in reasonably good agreement with the available experiments data on these molecules, as are the calculated fundamental frequencies. Relative to the CCSD(T) results, the GVB calculations yield bond distances that are too long by 0.015 Å in P_2 and 0.026 Å in As_2, and the calculated dissociation energies are too small by 39.75 kcal/mol (P_2) and 37.57 kcal/mol (As_2). In N_2, the GVB calculations recovered 76% of D_e[CCSD(T)]; in P_2 and As_2, the corresponding percentages are 65 and 57%, respectively, although the absolute errors are actually smaller in P_2 and As_2 than in N_2 (52.67 kcal/mol). It is interesting that the errors in D_e in P_2 and As_2 differ by just over 2 kcal/mol.

Table 5. Equilibrium Bond Distances (R_e), Bond Energies (D_e), Harmonic Vibrational Frequencies (ω_e), and Total Energy (E_e) for the Ground ($X^1\Sigma_g^+$) States of P_2 and As_2[a]

method	R_e (Å)	D_e (kcal/mol)	ω_e (cm^{-1})	E_e (au)
		P_2		
HF	1.850	40.10	913.8	−681.500595
GVB	1.917	73.24	732.3	−681.553419
val-CASSCF	1.920	96.80	756.4	−681.590964
MRCI+Q	1.906	112.74	771.9	−681.834858
CCSD(T)	1.902	112.99	782.6	−681.836373
Expt[b]	1.893	116.9	780.8	
		As_2		
HF	2.050	13.00	510.1	−662.440667
GVB	2.146	49.44	376.2	−662.498479
val-CASSCF	2.136	70.93	409.0	−662.532990
MRCI+Q	2.124	87.50	418.4	−662.744472
CCSD(T)	2.120	87.01	427.1	−662.744665
Expt[b]	2.103	92.0	429.5	

[a]Basis sets: aug-cc-pV(Q+d)Z (P_2) and aug-cc-pVQZ-PP (As_2). [b]Ref 9.

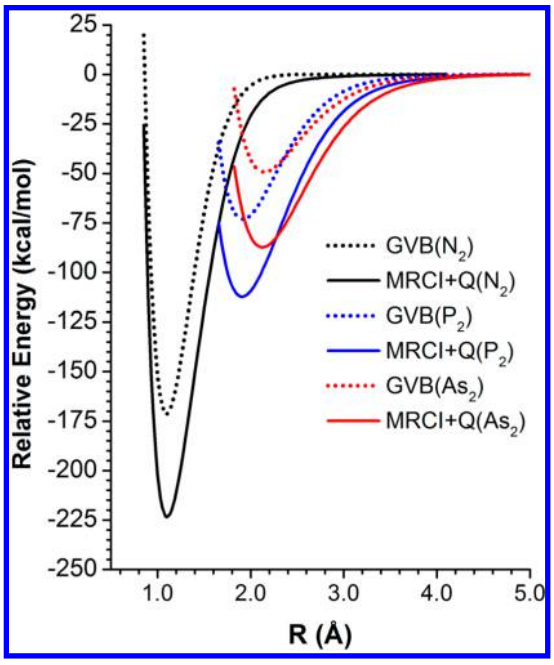

Figure 6. Composite potential energy curves for N_2, P_2, and As_2. Only the GVB and MRCI+Q curves are plotted for each molecule. Basis sets: aug-cc-pVQZ (N_2), aug-cc-pV(Q+d)Z (P_2), and aug-cc-pVQZ-PP (As_2).

3.3.2. Analysis of the GVB Wave Functions of P_2 and As_2. As noted in Section 2, the GVB wave functions of P_2 and As_2 have the same general form as N_2, differing only in the number of doubly occupied core orbitals. Although the spin functions are the same for any six-electron singlet state, the spatial orbitals, orbital overlaps, and spin function coefficients will be different for all three molecules. Thus, even though N_2, P_2, and As_2 are valence isoelectronic species, the nature of the bonding may be different.

Orbitals and Orbital Overlaps. Figure 7 shows the GVB orbitals for P_2 as a function of the internuclear distance, ΔR, with $\Delta R = R - R_e$ and R_e = 1.906 Å (the result from the MRCI calculation). Again, only four GVB active orbitals are shown. At large distances, ΔR = 2.0 Å, the GVB active orbitals are simply the atomic 3p orbitals on two P(^{4}S) atoms. As the distance decreases, the orbitals hybridize and delocalize into the bonding region. Compared to N_2, (φ_{a3}, φ_{a4}) appear to delocalize less onto the other atom but build in 3d character more strongly as the internuclear distance decreases. The doubly occupied 3s orbitals behave similarly to the 2s orbitals in N_2, polarizing away from the forming σ bond pair. The overlaps between the active orbitals are plotted in Figure 8 for all three molecules. At R_e, S_{12} = 0.88 (σ bonding orbitals) and S_{34} = 0.62 (π bonding orbitals) for P_2, compared to 0.89 and 0.69 for N_2. Both overlaps are smaller than those for N_2, especially S_{34}. The π orbitals (φ_{a3}, φ_{a4}) are clearly not able to overlap quite as effectively in P_2 as in N_2. Comparing the orbital overlap plots for P_2 with N_2, we see that the increase in S_{12} and S_{34} begins at a larger ΔR for P_2 than for N_2. This is a direct result of the much larger size of the phosphorus 3p orbital compared to the nitrogen 2p orbital ($\overline{r}_{3p} = 2.32a_0$ versus $\overline{r}_{2p} = 1.41a_0$).

Figure 9 shows the GVB orbitals of As_2 as a function the internuclear distance (again, only four of the six GVB active orbitals are shown). At long distances, ΔR = 2.0 Å, the GVB active orbitals are the atomic 4p orbitals on two As(^{4}S) atoms. As the distance decreases, the orbitals hybridize into the bonding region and delocalize onto the other atom. As in N_2 and P_2, the σ bonding orbitals (φ_{a1}, φ_{a2}) hybridize and delocalize more strongly as ΔR decreases. As in P_2, the π bonding orbitals (φ_{a3}, φ_{a4}) are less delocalized and build in a noticeable measure of 4d character as ΔR decreases. Comparing the orbital overlaps in

DOI: 10.1021/acs.jctc.5b00104
J. Chem. Theory Comput. 2015, 11, 2496−2507

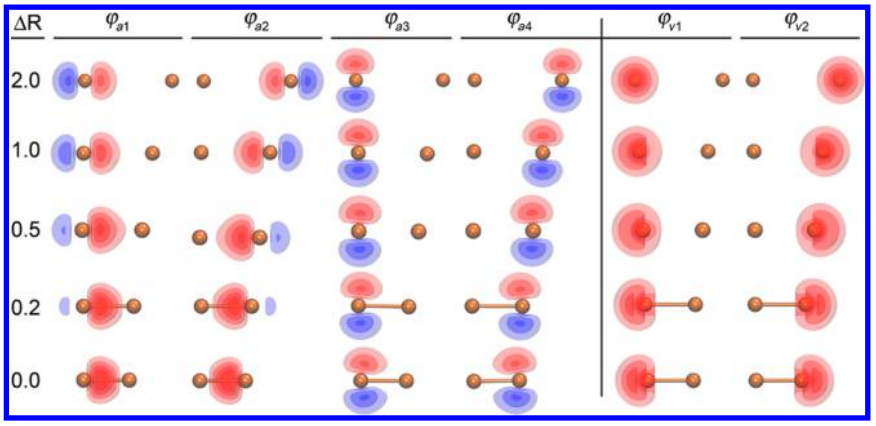

Figure 7. GVB orbitals of $P_2(X^1\Sigma_g^+)$ as a function of ΔR; $\Delta R = R - R_e$, R_e = 1.906 Å. The active GVB orbitals are on the left side of the vertical divider, and the doubly occupied valence orbitals are on the right side. Basis set: aug-cc-pV(Q+d)Z.

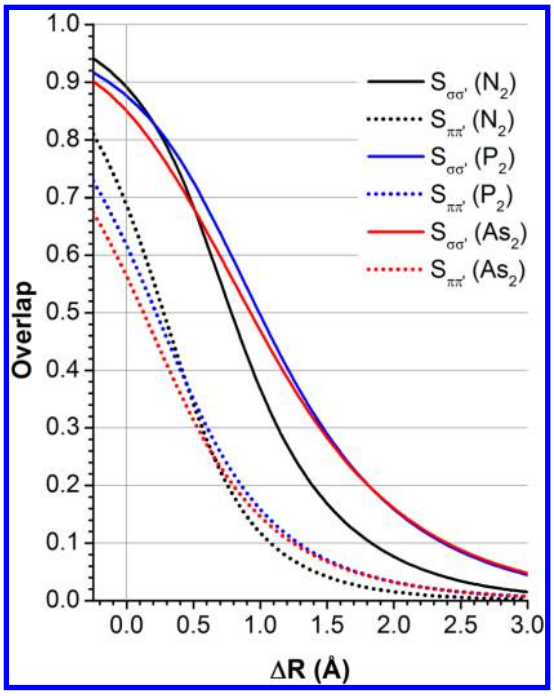

Figure 8. Orbital overlaps for the σ and π bonding orbitals of N_2, P_2, and As_2 as a function of $\Delta R = R - R_e$; R_e = 1.101 Å (N_2), 1.906 Å (P_2), and 2.124 Å (As_2).

Figure 8, we see that the π orbital overlap decreases noticeably going down the column in the periodic table. At R_e, S_{12} = 0.85 (σ) and S_{34} = 0.56 (π) for As_2, compared to 0.89 and 0.69 for N_2 and 0.88 and 0.62 for P_2. The difference between the overlaps of the σ and π bonding orbitals also increases down the column. It is 0.20 for N_2, 0.26 for P_2, and 0.29 for As_2. It is worthwhile noting that for the arsenic atom $\overline{r}_{4p} = 2.51a_0$; thus, the 4p orbital in arsenic is only about 10% larger than the 3p orbital in phosphorus, which correlates well with the similarity of the overlap plots for the σ and π orbitals of P_2 and As_2.

Spin Functions and Weights. Table 6 summarizes the results of the full and restricted GVB calculations for the three orbital orderings of the active orbitals for P_2 and As_2 at R_e. The dominant spin function weights for the molecular, quasi-atomic, and atomic ordering are 0.882, 0.859, and 0.821 for P_2 and 0.871, 0.873, and 0.830 for As_2. In comparison, the weights are 0.919, 0.841, and 0.772 for N_2. Thus, in both P_2 and As_2, the perfect pairing spin coupling is less important compared to the other two spin couplings, with the quasi-atomic spin coupling becoming more and more comparable to the molecular (perfect pairing) coupling, a direct reflection of the decreased overlap between the π bonding orbitals in P_2 and As_2. Even though the perfect pairing spin coupling still has the largest weight in P_2 and nearly the largest weight in As_2, it is clear that both of these species are beginning to deviate from the traditional single σ and double π bond description. In As_2, the molecular and quasi-atomic spin couplings are essentially equivalent.

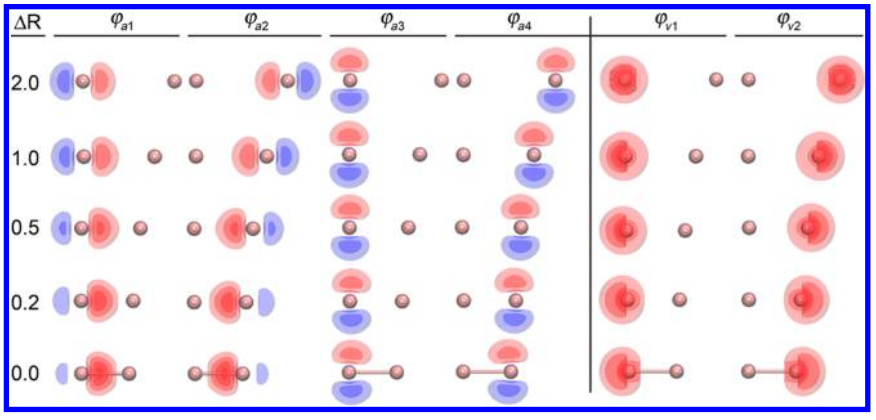

Figure 9. GVB orbitals of $As_2(X^1\Sigma_g^+)$ as a function of ΔR; $\Delta R = R - R_e$, R_e = 2.124 Å. GVB active orbitals are on the left side of the vertical divider, and doubly occupied valence orbitals are on the right side. Basis set: aug-cc-pVQZ-PP.

DOI: 10.1021/acs.jctc.5b00104
J. Chem. Theory Comput. 2015, 11, 2496−2507

Table 6. Energies, Spin Function Weights, Orbital Overlaps, and Energy Differences for the Three Orbital Orderings for P_2 and As_2 at R_e[a]

	molecular	quasi-atomic	atomic
		P_2	
E_{GVB} (au)		−681.553346	
$S_{\sigma\sigma}$		0.88	
$S_{\pi\pi}$		0.62	
w_k	0.882 (k = 5)	0.859 (k = 3)	0.821 (k = 1)
E_{rGVB} (au)	−681.547327	−681.544978	−681.545265
$S_{\sigma\sigma'}$	0.88	0.88	0.96
$S_{\pi\pi'}$	0.63	0.67	0.66
ΔE_{rGVB} (kcal/mol)	3.78	5.25	5.07
		As_2	
E_{GVB} (au)		−662.498289	
$S_{\sigma\sigma'}$		0.85	
$S_{\pi\pi'}$		0.56	
w_k	0.871 (k = 5)	0.873 (k = 3)	0.830 (k = 1)
E_{rGVB} (au)	−662.491513	−662.490601	−662.490017
$S_{\sigma\sigma'}$	0.83	0.83	0.95
$S_{\pi\pi'}$	0.58	0.61	0.61
ΔE_{rGVB} (kcal/mol)	4.25	4.82	5.19

[a] R_e = 1.906 Å (P_2) and 2.124 Å (As_2).

These changes in the weights of the various spin couplings are reflected in the energy differences, $\Delta E_{rGVB} = E_{rGVB} - E_{GVB}$. In N_2, these differences are 4.15 (*molecular*), 9.36 (*quasi-atomic*), and 10.55 kcal/mol (*atomic*). So, the perfect pairing spin function results in a significantly smaller error, relative to the full GVB energy, than the other two spin functions. In P_2, the differences are 3.78 (*molecular*), 5.25 (*quasi-atomic*), and 5.07 kcal/mol (*atomic*), and in As_2, they are 4.25 (*molecular*), 4.82 (*quasi-atomic*), and 5.19 kcal/mol (*atomic*). Clearly, the quasi-atomic coupling becomes more and more important progressing down the column.

The variations in the weights of the dominant spin functions for the molecular, quasi-atomic, and atomic orbital orderings are plotted as a function of the internuclear distance, ΔR, in Figure 10. (Note that because of the different orbital orderings used in the three GVB wave functions these weights do not sum to 1.) Although the functional dependence of the weights for P_2 and As_2 are similar to that for N_2, the steady growth in the importance of the quasi-atomic and atomic spin couplings from N_2 to As_2 is clearly evident in the figure. In addition, the curves shift to the left relative to R_e down the periodic table. Thus, in N_2, the atomic coupling dominates at large R, $\Delta R \gtrsim 0.5$ Å; the quasi-atomic coupling is only important in a relatively limited intermediate region, $\Delta R \approx 0.3-0.5$ Å; and the molecular coupling is dominant around R_e, $\Delta R < 0.3$ Å. At very short separations, $\Delta R < 0.0$ Å, the molecular coupling weight continues to increase as ΔR decreases, reaching a plateau, whereas those of the two other couplings decrease with decreasing ΔR. In P_2, the atomic spin coupling also has the largest weight at large R ($\Delta R \gtrsim 0.4$ Å), whereas the quasi-atomic spin coupling is most important in a somewhat larger intermediate region ($\Delta R \approx 0.1-0.4$ Å). Below $\Delta R \approx 0.1$ Å, the molecular (perfect pairing) spin coupling has the largest weight. In As_2, this trend continues. The atomic coupling is largest for $\Delta R \gtrsim 0.35$ Å, but, most importantly, the quasi-atomic coupling now dominates in the region from $\Delta R \approx 0.35$ Å to R_e. The molecular coupling becomes truly dominant only at distances shorter than R_e. Even then, the relative importance of the molecular coupling compared to the other two couplings is not as great as in N_2; the difference between the perfect pairing

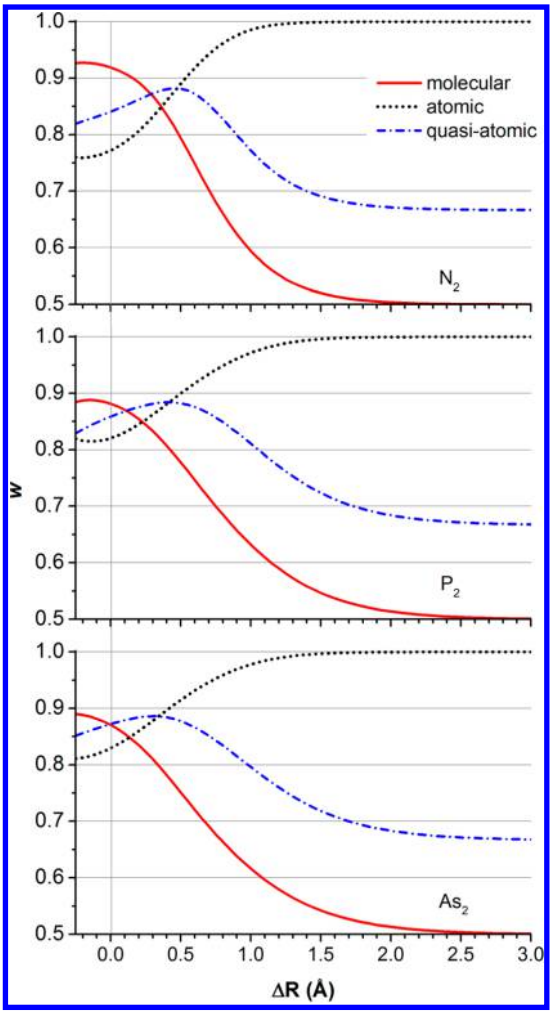

Figure 10. Dominant spin coupling weights for the three orbital orderings as a function of ΔR for N_2, P_2, and As_2. $\Delta R = R - R_e$; R_e = 1.101 Å (N_2), 1.906 Å (P_2), and 2.124 Å (As_2). Since different orbital orderings are used here, the three weights do not sum to 1.

DOI: 10.1021/acs.jctc.5b00104
J. Chem. Theory Comput. 2015, 11, 2496−2507

weight and the quasi-atomic weight decreases from N_2 to P_2 to As_2.

The changes in the spin coupling from N_2 to As_2, which is directly related to the smaller overlaps of the 3p and 4p orbitals, could also contribute to the weaker bonds in P_2 and As_2, especially weaker π bonds. These latter molecules have a much larger contribution from the quasi-atomic spin coupling and retain a larger contribution from the atomic spin coupling than does N_2. Thus, it is reasonable to view N_2 as possessing a triple bond, but P_2 and As_2 appear to have a somewhat more complicated bonding structure (although the difference is not as dramatic as in C_2). The increased importance of the quasi-atomic coupling could also impact the chemical reactivities of the heavier homologues of N_2; it should be easier to form bonds with the electrons in orbitals that are antiferromagnetically coupled than those that are singlet coupled.

4. CONCLUSIONS

Generalized valence bond (GVB) theory provides a more accurate, consistent, and detailed description of the electronic structure of molecules than does Hartree−Fock (HF) theory. The GVB wave function includes the most important nondynamical correlation effects in both the atoms and the molecule and, thus, provides a more consistent description of the electronic structure of molecules. For example, for both N_2 and C_2, the GVB wave function recovers 75−78% of the dissociation energies of these two molecules. In contrast, the HF wave function recovers slightly more than 50% of the bond energy of N_2 and only 13% of the bond energy of C_2.

The flexibility of the GVB wave function also allows a better understanding of the spin coupling of the electrons in the bonding orbitals in molecules. For most molecules, the perfect pairing spin coupling is dominant around the equilibrium geometry, which is consistent with the spin coupling assumed in the HF wave function. However, not all molecules can be so described. In fact, this is not the case in C_2. Forcing the electrons in C_2 to be paired into four singlet pairs increases the GVB energy by more than 20 kcal/mol. P_2 and As_2 represent intermediate cases.

For Pn_2, with six electrons directly involved in the bonding, there are five different spin couplings that must be considered. Three of these couplings are very important in describing the electronic structure of N_2, P_2, and As_2, as represented diagrammatically in Figure 11:

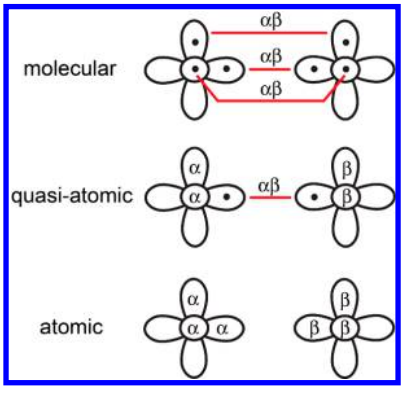

Figure 11. Diagrammatic representation of the three spin couplings in Pn_2. A red line denotes a singlet-coupled electron pair.

- *molecular coupling*, which is a product of three singlet spin functions (perfect pairing), describes a set of well-defined σ and π bonds;
- *quasi-atomic coupling*, which couples the two electrons in the σ bonding orbitals into a singlet and then couples the remaining electrons in the π orbitals into triplets as they are in the nitrogen atom, describes a well-defined σ bond, with weaker binding associated with the antiferromagnetic coupling of the electrons in the π orbitals; and
- *atomic coupling*, which couples all of the electrons, in both the σ and π orbitals, on each atom into quartets as they are in the separated atoms (full antiferromagnetic coupling); this represents the weakest binding at R_e with significant distortions of the associated GVB orbitals.

Which of these three couplings is dominant depends on the internuclear distance, with the atomic coupling being dominant at large R, the quasi-atomic coupling (which represents formation of a σ bond) being dominant at intermediate R, and the molecular coupling (which represents formation of a σ and two π bonds) being dominant around R_e.

It should be noted that, although the bond energies are larger for the molecular coupling in all three molecules, the bond energies are still quite large for both the quasi-atomic and atomic couplings. This is a direct result of the substantial overlaps between the bonding orbitals on the two pnictogen atoms.

The N_2 molecule is viewed as a prototype multiply bonded molecule with one σ bond and two π bonds. Indeed, the perfect pairing spin coupling with three singlet-coupled pairs has the largest weight by far at R_e, w_{PP} = 0.919, with this GVB configuration representing nearly 92% of the GVB wave function. Therefore, the GVB description of the bonding in N_2 is consistent with the usual triple bond assignment. At R_e, imposing the perfect pairing restriction raises the GVB energy by only slightly more than 4 kcal/mol. The remainder of the error in the dissociation energy of N_2, 57 kcal/mol, is due to dynamical correlation of the electrons.

The description of the bonding becomes somewhat more complicated as one proceeds down the Group 15 column from N_2 to As_2, largely as a result of the weaker overlap of the π bonding orbitals in P_2 and As_2. For P_2, the weight of the perfect pairing spin coupling is less that in N_2, 0.882 versus 0.919. In addition, the differences between the weights of the three spin couplings are smaller, with the molecular coupling having only a slightly larger weight than the quasi-atomic coupling, 0.882 versus 0.859, respectively. This trend continues in As_2, where the weights of the molecular and quasi-atomic couplings are essentially identical: 0.871 (*molecular*) versus 0.873 (*quasi-atomic*). It would be interesting to know if analyses such as that reported by Jerabek and Frenking,[54] which are currently based on the electron density, could be extended to include the effects of spin, since it is possible that the smaller bond energy of P_2 and As_2 relative to N_2 may be influenced by the increased importance of the quasi-atomic spin coupling in these two molecules.

■ ASSOCIATED CONTENT

Supporting Information

Spin coupling weights of N_2 as a function of ΔR in the quasi-atomic and atomic orbital ordering, as well as the spin coupling weights of P_2 and As_2 as a function of ΔR in the molecular, quasi-atomic, and atomic orbital ordering. Comparison of the HF and GVB orbitals at R_e, as well as the five spin basis functions. The

DOI: 10.1021/acs.jctc.5b00104
J. Chem. Theory Comput. 2015, 11, 2496−2507

Supporting Information is available free of charge on the ACS Publications website at DOI: 10.1021/acs.jctc.5b00104.

AUTHOR INFORMATION

Corresponding Author

*E-mail: thdjr@uw.edu; thom.dunning@pnnl.gov.

Present Address

†(L.T.X. and T.H.D., Jr.) Northwest Institute for Advanced Computing (NIAC), Pacific Northwest National Laboratory, c/o University of Washington, Sieg Hall, Room 127, 3960 Benton Lane NE, Seattle, Washington 98195, United States.

Funding

This work was supported by funding from the Distinguished Chair for Research Excellence in Chemistry and the National Center for Supercomputing Applications at the University of Illinois at Urbana−Champaign.

Notes

The authors declare no competing financial interest.

ACKNOWLEDGMENTS

We thank the other members of our research group for their valuable comments on the material presented herein.

REFERENCES

(1) Su, P.; Wu, J.; Gu, J.; Wu, W.; Shaik, S.; Hiberty, P. C. Bonding Conundrums in the C_2 Molecule: A Valence Bond Study. *J. Chem. Theory Comput.* **2011**, *7*, 121−130.

(2) Shaik, S.; Danovich, D.; Wu, W.; Su, P.; Rzepa, H. S.; Hiberty, P. C. Quadruple Bonding in C_2 and Analogous Eight-Valence Electron Species. *Nat. Chem.* **2012**, *4*, 195−200.

(3) Shaik, S.; Rzepa, H. S.; Hoffmann, R. One Molecule, Two Atoms, Three Views, Four Bonds? *Angew. Chem., Int. Ed.* **2013**, *52*, 3020−3033.

(4) Frenking, G.; Hermann, M. Critical Comments on "One Molecule, Two Atoms, Three Views, Four Bonds?". *Angew. Chem., Int. Ed.* **2013**, *52*, 5922−5925.

(5) Danovich, D.; Shaik, S.; Rzepa, H. S.; Hoffmann, R. A Response to the Critical Comments on "One Molecule, Two Atoms, Three Views, Four Bonds?". *Angew. Chem., Int. Ed.* **2013**, *52*, 5926−5928.

(6) Danovich, D.; Hiberty, P. C.; Wu, W.; Rzepa, H. S.; Shaik, S. The Nature of the Fourth Bond in the Ground State of C_2: The Quadruple Bond Conundrum. *Chem.—Eur. J.* **2014**, *20*, 6220−6232.

(7) Mulliken, R. S. Note on Electronic States of Diatomic Carbon, and the Carbon−Carbon Bond. *Phys. Rev.* **1939**, *56*, 778−781.

(8) Xu, L. T.; Dunning, T. H., Jr. Insights Into the Perplexing Nature of the Bonding in C_2 From Generalized Valence Bond Calculations. *J. Chem. Theory Comput.* **2014**, *10*, 195−201.

(9) Huber, K. P.; Herzberg, G. *Molecular Spectra and Molecular Structure: Constants of Diatomic Molecules*; Prentice-Hall: New York, 1979; Vol. *IV*.

(10) Tofan, D.; Cummins, C. C. Photochemical Incorporation of Diphosphorus Units into Organic Molecules. *Angew. Chem., Int. Ed.* **2010**, *49*, 7516−7518.

(11) Wang, Y.; Xie, Y.; Wei, P.; King, R. B.; Schaefer, H. F., III; Schleyer, P. v. R.; Robinson, G. H. Carbene-Stabilized Diphosphorus. *J. Am. Chem. Soc.* **2008**, *130*, 14970−14971.

(12) Huttner, G.; Sigwarth, B.; Scheidsteger, O.; Zsolnai, L.; Orama, O. Diarsenic, As_2, as a Four-, Six-, or Eight-Electron Donor Ligand. *Organometallics* **1985**, *4*, 326−332.

(13) Schwarzmaier, C.; Timoshkin, A. Y.; Scheer, M. An End-on-Coordinated As_4 Tetrahedron. *Angew. Chem., Int. Ed.* **2013**, *52*, 7600−7603.

(14) Dunning, T. H., Jr.; Cartwright, D. C.; Hunt, W. J.; Hay, P. J.; Bobrowicz, F. W. Generalized Valence Bond Calculations on the Ground State ($X^1\Sigma_g^+$) of Nitrogen. *J. Chem. Phys.* **1976**, *64*, 4755−4766.

(15) Goddard, W. A., III Improved Quantum Theory of Many-Electron Systems. II. The Basic Method. *Phys. Rev.* **1967**, *157*, 81−93.

(16) Goddard, W. A., III; Dunning, T. H., Jr.; Hunt, W. J.; Hay, P. J. Generalized Valence Bond Description of Bonding in Low-Lying States of Molecules. *Acc. Chem. Res.* **1973**, *6*, 368−376.

(17) Roos, B. O. The Complete Active Space SCF Method in a Fock-Matrix-Based Super-CI Formulation. *Int. J. Quantum Chem.* **1980**, *18*, 175−189.

(18) Ruedenberg, K.; Schmidt, M. W.; Gilbert, M. M.; Elbert, S. T. Are Atoms Intrinsic to Molecular Electronic Wavefunctions? I. The FORS Model. *Chem. Phys.* **1982**, *71*, 41−49.

(19) Werner, H.-J.; Knowles, P. J. A Second Order Multiconfiguration SCF Procedure with Optimum Convergence. *J. Chem. Phys.* **1985**, *82*, 5053−5063.

(20) Knowles, P. J.; Werner, H.-J. An Efficient Second-Order MCSCF Method for Long Configuration Expansions. *Chem. Phys. Lett.* **1985**, *115*, 259−267.

(21) Werner, H.-J.; Knowles, P. J. An Efficient Internally Contracted Multiconfiguration Reference Configuration-Interaction Method. *J. Chem. Phys.* **1988**, *89*, 5803−5814.

(22) Knowles, P. J.; Werner, H.-J. An Efficient Method for the Evaluation of Coupling Coefficients in Configuration Interaction Calculations. *Chem. Phys. Lett.* **1988**, *145*, 514−522.

(23) Shamasundar, K. R.; Knizia, G.; Werner, H.-J. A New Internally Contracted Multi-reference Configuration Interaction Method. *J. Chem. Phys.* **2011**, *135*, 054101.

(24) Langhoff, S. R.; Davidson, E. R. Configuration Interaction Calculations on the Nitrogen Molecule. *Int. J. Quantum Chem.* **1974**, *8*, 61−72.

(25) Purvis, G. D., III; Bartlett, R. J. A Full Coupled-Cluster Singles and Doubles Model: The Inclusion of Disconnected Triples. *J. Chem. Phys.* **1982**, *76*, 1910−1918.

(26) Hampel, C.; Peterson, K. A.; Werner, H.-J. A Comparison of the Efficiency and Accuracy of the Quadratic Configuration Interaction (QCISD), Coupled Cluster (CCSD), and Brueckner Coupled Cluster (BCCD) Methods. *Chem. Phys. Lett.* **1992**, *190*, 1−12.

(27) Deegan, M.; Knowles, P. J. Perturbative Corrections To Account for Triple Excitations in Closed and Open-Shell Coupled-Cluster Theories. *Chem. Phys. Lett.* **1994**, *227*, 321−326.

(28) Dunning, T. H., Jr. Gaussian Basis Sets for Use in Correlated Molecular Calculations. I. The Atoms Boron through Neon and Hydrogen. *J. Chem. Phys.* **1989**, *90*, 1007.

(29) Dunning, T. H., Jr.; Peterson, K. A.; Wilson, A. K. Gaussian Basis Sets for Use in Correlated Molecular Calculations. X. The Atoms Aluminum through Argon Revisited. *J. Chem. Phys.* **2001**, *114*, 9244−9253.

(30) Peterson, K. A. Systematically Convergent Basis Sets with Relativistic Pseudopotentials. I. Correlation Consistent Basis Sets for the Post-D Group 13−15 Elements. *J. Chem. Phys.* **2003**, *119*, 11099−11112.

(31) Werner, H.-J.; Knowles, P. J.; Amos, R. D.; Bernhardsson, A.; Berning, A.; Celani, P.; Cooper, D. L.; Deegan, M. J. O.; Dobbyn, A. J.; Eckert, F.; Hampel, C.; Hetzer, G.; Korona, T.; Lindh, R.; Lloyd, A. W.; McNicholas, S. J.; Manby, F. R.; Meyer, W.; Mura, M. E.; Nicklass, A.; Palmieri, P.; Pitzer, R.; Rauhut, G.; Schütz, M.; Schumann, U.; Stoll, H.; Stone, A. J.; Tarroni, R.; Thorsteinsson, T.; Wang, M. *Molpro*, version 2010.1, a Package of *Ab Initio* Programs; University College Cardiff Consultants Limited: Wales, UK; http://www.molpro.net.

(32) Werner, H.-J.; Knowles, P. J.; Knizia, G.; Manby, F. R.; Schütz, M. Molpro: A General-Purpose Quantum Chemistry Program Package. *Wiley Interdiscip. Rev.: Comput. Mol. Sci.* **2011**, *2*, 242−253.

(33) Dunning, T. H., Jr.; Woon, D. E.; Leiding, J.; Chen, L. The First Row Anomaly and Recoupled Pair Bonding in the Halides of the Late P-Block Elements. *Acc. Chem. Res.* **2013**, *46*, 359−368.

(34) Dunning, T. H., Jr.; Xu, L. T.; Takeshita, T. Y. Fundamental Aspects of Recoupled Pair Bonds. I. Recoupled Pair Bonds in Carbon and Sulfur Monofluoride. *J. Chem. Phys.* **2015**, *142*, 034113.

(35) Dunning, T. H., Jr.; Takeshita, T. Y.; Xu, L. T. Fundamental Aspects of Recoupled Pair Bonds. II. Recoupled Pair Bond Dyads in Carbon and Sulfur Difluoride. *J. Chem. Phys.* **2015**, *142*, 034114.

(36) Penotti, F. E.; Cooper, D. L. Combining Symmetry-Separated and Bent-Bond Spin-Coupled Models of Cylindrically Symmetric Multiple Bonding. *Mol. Phys.* **2015**, 1−5.
(37) Kotani, M. On the Valence Theory of the Methane Molecule. *Proc. Phys.-Math. Soc. Jpn.* **1937**, *19*, 460−470.
(38) Kotani, M. Note on the Theory of Electronic State of Polyatomic Molecules. *Proc. Phys.-Math. Soc. Jpn.* **1938**, *19*, 471.
(39) Karadakov, P.; Gerratt, J.; Cooper, D.; Raimondi, M. SPINS: A Collection of Algorithms for Symbolic Generation and Transformation of Many-Electron Spin Eigenfunctions. *Theor. Chim. Acta* **1995**, *90*, 51−73.
(40) Raos, G.; Gerratt, J.; Cooper, D. L.; Raimondi, M. On the Role of Different Spin Bases within Spin-Coupled Theory. *Mol. Phys.* **1993**, *79*, 197−216.
(41) Gerratt, J.; Lipscomb, W. N. Spin-Coupled Wave Functions for Atoms and Molecules. *Proc. Natl. Acad. Sci. U.S.A.* **1968**, *59*, 332−335.
(42) Gerratt, J. General Theory of Spin-Coupled Wave Functions for Atoms and Molecules. *Adv. At. Mol. Phys.* **1971**, *7*, 141−221.
(43) Gerratt, J.; Cooper, D. L.; Karadakov, P. B.; Raimondi, M. Modern Valence Bond Theory. *Chem. Soc. Rev.* **1997**, *26*, 87−100.
(44) Thorsteinsson, T.; Cooper, D. L.; Gerratt, J.; Karadakov, P.; Raimondi, M. Modern Valence Bond Representations of CASSCF Wavefunctions. *Theor. Chim. Acta* **1996**, *93*, 343−366.
(45) Cooper, D. L.; Thorsteinsson, T.; Gerratt, J. Fully Variational Optimization of Modern VB Wave Functions Using the CASVB Strategy. *Int. J. Quantum Chem.* **1997**, *65*, 439−451.
(46) Cooper, D. L.; Thorsteinsson, T.; Gerratt, J. Modern VB Representations of CASSCF Wave Functions and the Fully-Variational Optimization of Modern VB Wave Functions Using the CASVB Strategy. *Adv. Quan. Chem.* **1998**, *32*, 51−67.
(47) Thorsteinsson, T.; Cooper, D. L. An Overview of the CASVB Approach to Modern Valence Bond Calculations. In *Quantum Systems in Chemistry and Physics: Basis Problems and Model Systems*; Hernandez-Laguna, A., Maruani, J., McWeeny, R., Wilson, S., Eds.; Kluwer: Dordrecht, 2000; Vol. *1*, pp 303−326.
(48) Werner, H.-J.; Knowles, P. J. Accurate Multireference Configuration Interaction Calculations of the Potential Energy Function and the Dissociation Energy of N_2. *J. Chem. Phys.* **1991**, *94*, 1264−1270.
(49) Sando, K. M. Spin-Projected and Extended SCF Calculations. *J. Chem. Phys.* **1967**, *47*, 180−185.
(50) Merritt, J. M.; Bondybey, V. E.; Heaven, M. C. Beryllium Dimer—Caught in the Act of Bonding. *Science* **2009**, *324*, 1548−1551.
(51) Goodgame, M. M.; Goddard, W. A. The "Sextuple" Bond of Cr_2. *J. Phys. Chem.* **1981**, *85*, 215−217.
(52) Goodgame, M. M.; Goddard, W. A., III Modified Generalized Valence-Bond Method: A Simple Correction for the Electron Correlation Missing in Generalized Valence-Bond Wave-Functions; Prediction of Double-Well States for Cr_2 and Mo_2. *Phys. Rev. Lett.* **1985**, *54*, 661−664.
(53) Kutzelnigg, W. Chemical Bonding in Higher Main Group Elements. *Angew. Chem., Int. Ed. Engl.* **1984**, *23*, 272−295.
(54) Jerabek, P.; Frenking, G. Comparative Bonding Analysis of N_2 and P_2 versus Tetrahedral N_4 and P_4. *Theor. Chim. Acta* **2014**, *133*, 1447−1449.

DOI: 10.1021/acs.jctc.5b00104
J. Chem. Theory Comput. 2015, 11, 2496−2507